



Bacteria encapsulation into polyethylene glycol hydrogels using Michael-type addition reactions

Moises M. Gutierrez¹ · Jeffrey A. Reed¹ · Robby A. McElroy¹ · Ryan R. Hansen¹

Received: 19 June 2024 / Accepted: 30 August 2024
© The Author(s) 2024

Abstract

Hydrogel materials can be used to integrate bacteria cells into biohybrid systems. Here, we investigate the use of polyethylene glycol-based hydrogels that employ different Michael-type addition crosslinking chemistries, including thiol-acrylate, thiol-vinyl sulfone, and thiol-maleimide click reactions, for covalent hydrogel network formation and bacteria encapsulation. All crosslinking chemistries generated hydrogels that provided stable encapsulation and culture of *Bacillus subtilis*; however, significant differences in cell viability and cell morphology after encapsulation were identified. Thiol-acrylate hydrogels provided the highest cell viability and favored encapsulation of single cells, while thiol-maleimide hydrogels had the lowest cell viability and favored encapsulation of larger aggregates. These findings demonstrate the impact of crosslinking strategies for encapsulation of microorganisms into hydrogel networks and suggest that thiol-acrylate chemistries are favorable for many applications.

Introduction

Encapsulation of microorganisms within hydrogel materials has proven to be an effective strategy for preserving cellular function and for providing controlled cell release, enabling advancements in probiotics [1], agriculture [2], and environmental applications [3]. Recent progress in synthetic biology has also facilitated the field of living materials, where a primary focus is on use of engineered cells to provide programmable control of material properties [4]. Prominent examples of living materials use embedded microorganisms to modulate hydrogel properties [5, 6]. These emerging research areas highlight the importance of hydrogel chemistries to provide stable encapsulation of viable bacteria.

The majority of hydrogels used for microorganism encapsulation employ naturally occurring polysaccharide-based materials, most notably alginate, chitosan, cellulose, starch, and hyaluronic acid. While used less frequently, synthetic hydrogels such as poly(ethylene glycol) (PEG), poly(vinyl alcohol), and poly(acrylamide) hold unique advantages over their naturally occurring counterparts, particularly with respect to their flexible design options to achieve a wide

range of tailored physicochemical properties. For example, hydrogels that use covalent PEG networks can be generated from a variety of commercially available PEG macromers with different end-group chemistries and molecular weights to yield highly tunable mesh sizes for control of mass transport [7]. Novel PEG macromers can also be used to generate hydrogels that are responsive to environmental stimuli, such as light, pH, or enzymatic activity [8], enabling dynamic control of the cellular microenvironment or triggered release of microorganisms at a desired time and location [9, 10]. Microbial encapsulation with PEG-based hydrogels have enabled recent advancements in anaerobic wastewater treatment systems [11, 12], bioelectrochemical systems [13], and selection of bacteria from microbial communities or culture collections [14–16].

A variety of chain and step-growth polymerization strategies can be used to generate covalent PEG hydrogel networks. Step-growth polymerization mechanisms that use click reactions for covalent crosslinking, which include thiol-ene, copper-catalyzed, and ring strain promoted azide-alkyne cycloaddition, inverse electron demand Diels–Alder cycloaddition, and Michael addition, can provide near stoichiometric conversion of crosslinking moieties for uniform network structure and precise control of hydrogel properties [17, 18]. While these novel crosslinking chemistries have received extensive use in tissue engineering and drug delivery, little attention has been given to its potential use for

✉ Ryan R. Hansen
rrhansen@ksu.edu

¹ Tim Taylor Department of Chemical Engineering, Kansas State University, Manhattan, KS, USA

microorganism encapsulation. Michael addition relies on base-catalyzed conjugate addition between a thiolate anion and an electron-deficient vinyl group [19] and is an attractive option for microbe encapsulation as it does not generate free radicals or require initiators and external energy input for initiation, does not generate side products, and does not require catalysts that have antimicrobial properties. Finally, unlike free radical polymerizations, Michael addition coupling reactions are insensitive to oxygen [19], making them equally amenable to encapsulation of aerobic and anaerobic microorganisms.

Here, we investigate the effects of crosslinking chemistry on bacteria encapsulation in PEG hydrogels when using three common Michael acceptors (acrylate, vinyl sulfone, and maleimide) present on difunctional PEG macromers. All groups are coupled with tetrafunctional PEG-thiol crosslinkers and use macromers with equivalent molecular weights to decipher the effects of end-group chemistry on bacteria encapsulation, cell viability, and growth (Fig. 1). *Bacillus subtilis* was used as a model bacteria as it is genetically tractable, produces endospores, and can provide host benefits in several biosystems, including the gut, plant rhizosphere, and soil. Encapsulated *B. subtilis* has garnered recent attention for controlled delivery [20, 21] and living hydrogel applications [22].

Materials and methods

Preparation of hydrogel precursor solutions and cell encapsulation

Bacillus subtilis or *B. subtilis* cells expressing GFP (*B. subtilis*-GFP) cells were grown in tryptic soy broth (TSB) at 28 °C for 24 h (hrs), followed by dilution into 2X ATGN minimal growth media in phosphate buffer (PBS) [23] to an optical density (OD₆₀₀) of 0.1. Hydrogel precursor solutions consisted of cultured *B. subtilis*, a four-armed PEG-thiol crosslinker (10-kDa PEGTT, 20 mM) and PEG

diacrylate (3.4-kDa PEGDA, 49 mM), PEG vinyl sulfone (3.4-kDa PEGVS, 49 mM), or PEG maleimide (3.4-kDa PEGMA, 49 mM) macromers to form PEG diacrylate-PEG tetrathiol (PEGDA-PEGTT), PEG vinyl sulfone-PEG tetrathiol (PEGVS-PEGTT), and PEG maleimide-PEG tetrathiol (PEGMA-PEGTT) hydrogels, respectively. Hydrogel precursor solutions were prepared by first mixing *B. subtilis* with the difunctional PEG macromer and then combining the solution with PEGTT incubating over thiolated glass coverslips for microscopic imaging, following the procedure described by Fattahi et al. [24]. More details on this experimental protocol are provided in the Supplementary Material file. A minimum of three independent replicates were made for each hydrogel. Average hydrogel mesh size for each hydrogel was measured as described by Canal and Peppas [25] and is further described in the Supplementary Material file (Table S1).

Characterization of cell morphology and viability

Cell morphology and viability immediately after bacteria-hydrogel encapsulation were characterized using an inverted fluorescent microscope (Nikon Eclipse Ti-E). For cell morphology studies, *B. subtilis*-GFP was used for fluorescence imaging. ImageJ 1.54 Analysis Particle tool was used to quantify the cell aggregate sizes. Histogram plots with a bin size of 7 μm² were generated from the raw data; a final bin of > 25 μm² was used for all larger aggregates. *B. subtilis* (non-GFP) was used for cell viability studies. Here, cells in each hydrogel were stained using a live/dead assay (Bacterial Viability Kit L7012). The percentage of live cells was determined by measuring the ratio of integrated green to red fluorescence intensity (R_{G/R}) and using the live-dead calibration curve (Fig. S1), following the manufacturer's recommended protocol [26]. All microscopic characterizations were performed for n ≥ 3 independent replicates.

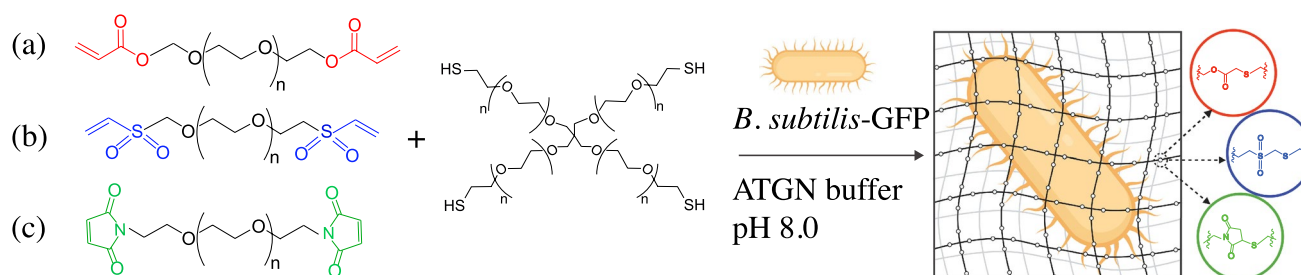


Fig. 1 Encapsulation of *B. subtilis*-GFP into PEG hydrogels using tetrafunctional PEG-thiol crosslinkers ($M_w=10$ kDa) and **a** PEG diacrylate, **b** PEG divinyl sulfone, or **c** PEG dimaleimide macromers ($M_w=3.4$ kDa), forming thioether ester (red), thioether sulfone

(blue), or succinimide thioether (green) bonds, respectively, at each crosslink through Michael addition. Figure was prepared with assistance from Biorender software

Bacteria growth kinetics

Kinetic growth studies were performed by encapsulating *B. subtilis*-GFP in hydrogels at the bottom of 96-well plate readers using the same monomer formulations as before but at 50- μL volumes. After hydrogel formation, 200 μL of ATGN minimal growth media was dispensed on top of the hydrogels, and cell growth was tracked by monitoring optical density (OD_{600}) for 72 h at 28 $^{\circ}\text{C}$ (Epoch2 Microplate Reader, Biotek). To verify that the measured cell growth was due to cells confined in the hydrogel and not due to cell growth in external growth media, 300 μL was sampled from the supernatant growth media every 10–12 h for OD_{600} measurement.

Statistical analysis

All statistical analyses were made using statistical software (SAS Institute Inc.). Mean and standard deviation were estimated based on a minimum of three independent replicates. Student *t* tests were used to compare datasets and determine statistical differences. A *p* value < 0.05 was considered statistically significant.

Results and discussion

The encapsulation and resulting morphology of *B. subtilis*-GFP cells into PEGDA-PEGTT, PEGVS-PEGTT, and PEGMA-PEGTT hydrogels were first investigated, and cell aggregation levels in each hydrogel were compared (Fig. 2A). Assuming an average diameter and length of a *B. subtilis* cell to be 1 and 2–6 μm , respectively [27], it can be estimated that particles with areas greater than $\sim 19 \mu\text{m}^2$ represent aggregated cells, while particles with lower areas represent individual cells or only a small number of cells. Lowest levels of aggregation were identified in PEGDA-PEGTT hydrogels. Here, the majority of particles fell into the lowest size range (0–7 μm^2), indicating individual cells. This was different than PEGMA-PEGTT hydrogels, where a significant decrease in particle numbers was identified at this size range (Fig. 2B). No significant differences were found across the three hydrogels for larger particle sizes; however, comparison of the percent of particles falling into each size category demonstrates the shifting particle size distribution (Fig. 2C). For PEGDA-PEGTT hydrogels, only 20.9% of particles were representative of aggregates ($> 19 \mu\text{m}^2$). A shift toward higher aggregation levels is noted in PEGVS-PEGTT hydrogels; here, 28.2% of particles represented aggregated cells, while PEGMA-PEGTT hydrogels showed a further shift to 31.1% of aggregated particles. In addition, sub-millimeter heterogeneities in cell distribution

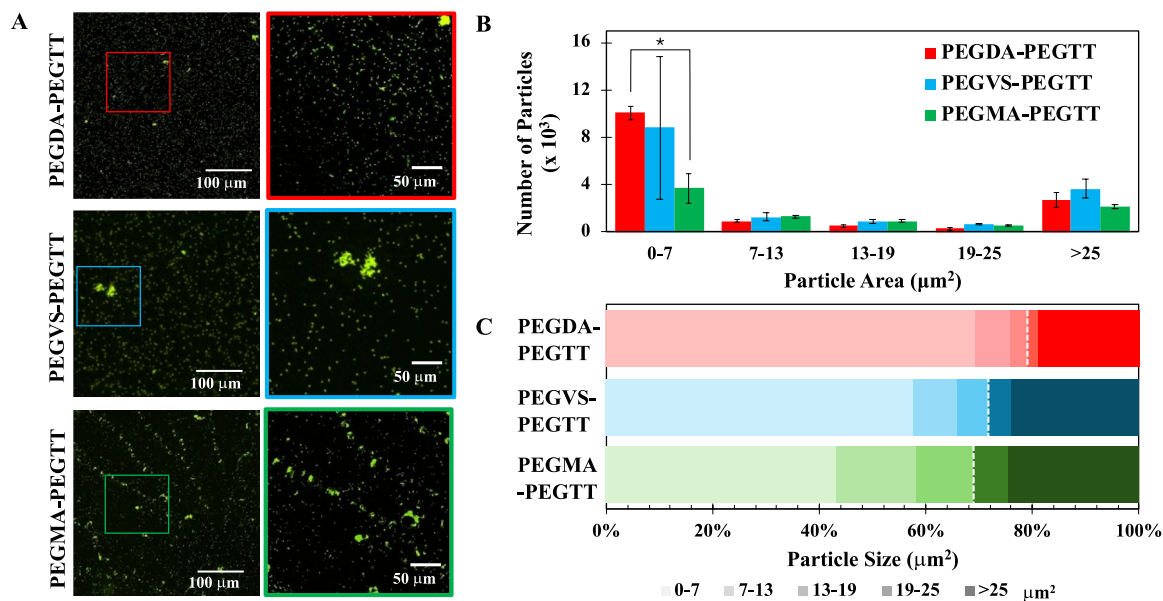


Fig. 2 Cell morphology after encapsulation in PEG hydrogels. **A** Representative 10X (left column) and 20X (right column) fluorescent images of *B. subtilis*-GFP cells after encapsulation into PEGDA-PEGTT, PEGVS-PEGTT, and PEGMA-PEGTT hydrogels. **B** Average number and **C** percentage of encapsulated bacteria falling into

size categories after particle size analysis ($*p < 0.05$). Darker shading in **C** indicates a larger particle size range. Dashed white line in **C** represent the cut-off area above which all particles are cellular aggregates. 10X images were used to quantify cell aggregation levels. Contrast was adjusted in Fig. 2A to improve visualization

were observed across PEGMA-PEGTT hydrogels, whereas cell distribution in PEGDA-PEGTT and PEGVS-PEGTT hydrogels appeared relatively uniform (Fig. 2A).

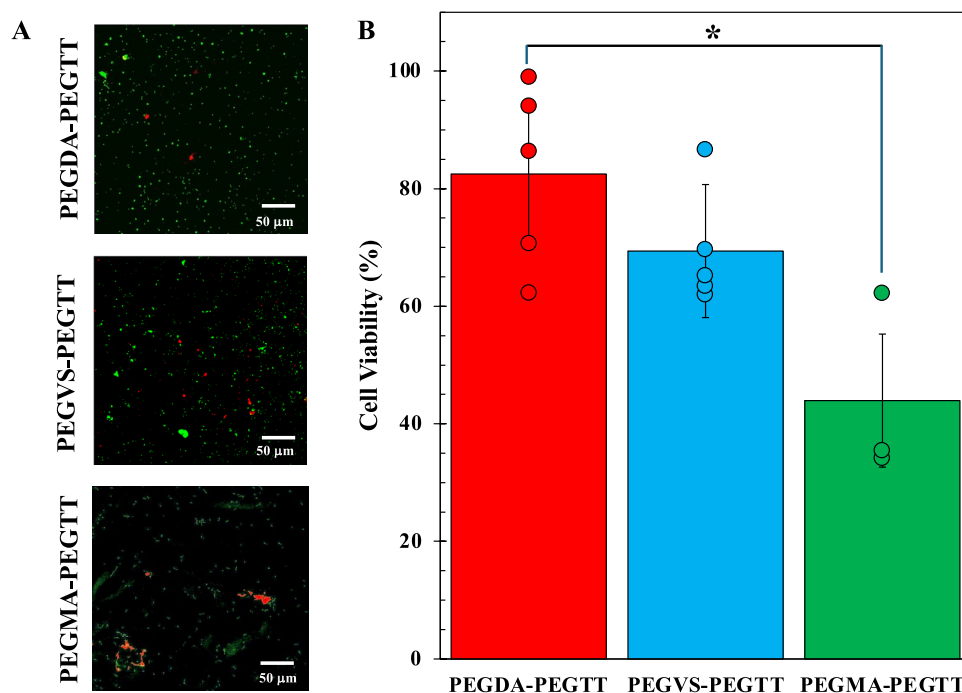
We hypothesized that the differences in aggregation levels were due to the reactivity of the different Michael acceptors toward thiol groups. Maleimide-thiol reaction kinetics are rapid, while vinyl sulfone-thiol and then acrylate-thiol reaction kinetics are successively slower [19, 28]. Fast gelation times of less than 6 s were observed when forming PEGMA-PEGTT hydrogels, which limited mixing to cause higher levels of crosslinking heterogeneity and non-uniform cell distribution, ultimately leading to bacterial aggregation. Similar trends have been noted when using thiol-maleimide crosslinking strategies to encapsulate mammalian cell lines in tissue culture applications [29]. The higher reactivity of the difunctional maleimides can also lead to cross-reactivity with native thiols present on the cell surface [30] or in the extracellular polymer substance (e.g., cysteine residues), which may also be a contributing factor to aggregation. By contrast, PEGVS-PEGTT hydrogels showed more uniform dispersion of bacteria throughout the hydrogel and PEGDA-PEGTT hydrogels, which required ~25 min for gelation, showed highest uniformity, which is potentially advantageous in applications where controlled release of beneficial bacteria is desired.

Live-dead staining of *B. subtilis* encapsulated in PEGDA-PEGTT, PEGVS-PEGTT, and PEGMA-PEGTT hydrogels revealed variations in cell viability (Fig. 3). Cell viability decreased with increased Michael acceptor reactivity, with PEGDA-PEGTT showing highest cell viability, followed

by PEGVS-PEGTT hydrogels, where lower but statistically equivalent cell viability was found. However, PEGMA-PEGTT hydrogels did show a statistically significant decrease when compared to PEGDA-PEGTT hydrogels. These trends are again comparable to tissue culture studies, where reactive crosslinking groups can have varied effects on cell toxicity due to cross-reactivity with mammalian cell lines [28] and where high cytotoxicity of maleimide crosslinkers has been reported [30]. Interestingly, many dead *B. subtilis* cells appeared within larger aggregates as opposed to single cells (Fig. 3A, PEGMA-PEGTT), again suggesting that cellular cross-reactivity and resulting cell aggregation were a cause of cytotoxicity in this system. By contrast, the uniform cell distributions within PEGDA-PEGTT hydrogels, as noted previously, appeared to promote cell survival.

Finally, as cell growth within hydrogels is a pre-requisite for most applications, the growth kinetics of encapsulated *B. subtilis* within the different hydrogels was studied. Here, *B. subtilis* was encapsulated into the respective hydrogels, and growth was monitored in 96-well plate format. Multiple controls were included for comparison. The first was culture of non-encapsulated *B. subtilis* present in bulk culture media (no hydrogel) of equivalent volume, which was used to decipher the effects of hydrogel confinement on growth. Second, free liquid media above *B. subtilis*-loaded hydrogel was sampled at 10–12-h increments during culture to check for release of cells from the hydrogel into the supernatant solution. A final set of control samples included empty hydrogels to decipher any interference of the hydrogels on the optical

Fig. 3 *B. subtilis* cell viability after hydrogel encapsulation. **A** Representative green–red fluorescent images of *B. subtilis* after encapsulation and live-dead staining (green denotes live cells, red denotes dead cells). **B** Quantified cell viabilities ($*p < 0.05$). Contrast was adjusted in Fig. 3A to improve visualization



density measurement. OD_{600} readings in empty hydrogels during exposure to growth media remained unchanged through the entire experiment, indicating no interference or growth from contaminant microorganisms (Fig. S2).

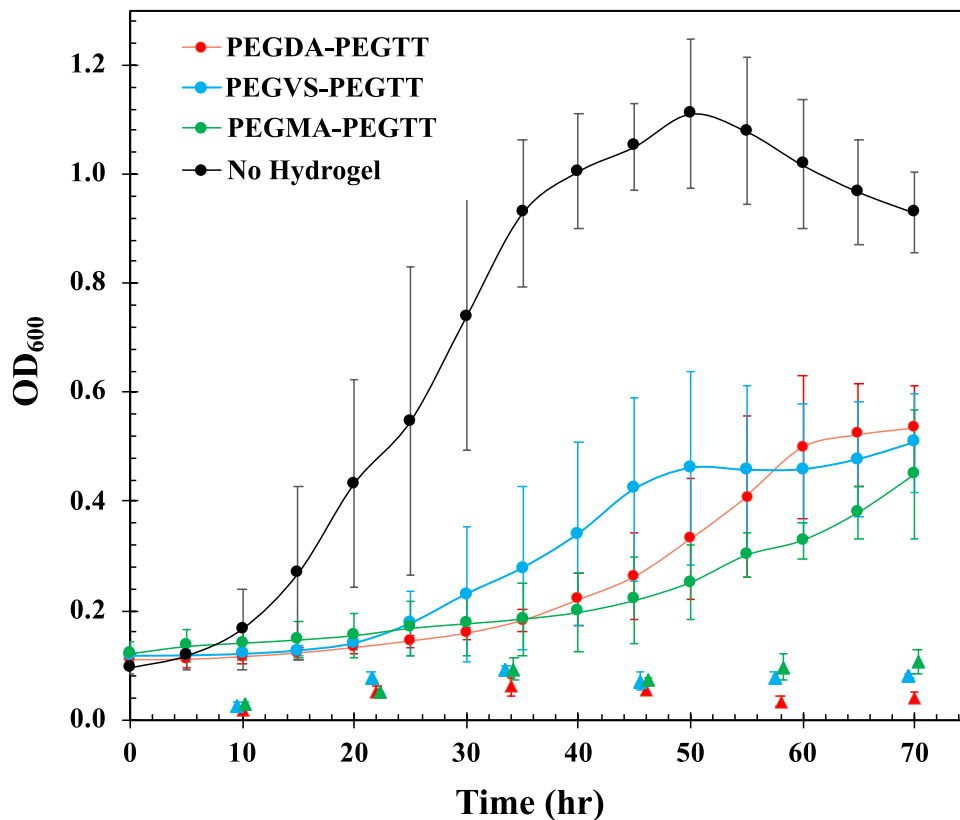
Hydrogel-encapsulated bacteria showed significant differences in growth kinetics and final growth levels compared to bacteria in bulk solution (Fig. 4). Increases in the lag phase were noted for bacteria encapsulated in all hydrogels (lag phase: no hydrogel = 12.5 h; PEGDA-PEGTT = 33.6 h; PEGVS-PEGTT = 22.6 h; PEGMA-PEGTT = 42.3 h), as well as decreases in exponential phase growth rates (growth rate: no hydrogel = 0.129 h^{-1} ; PEGDA-PEGTT = 0.060 h^{-1} ; PEGVS-PEGTT = 0.096 h^{-1} ; PEGMA-PEGTT = 0.055 h^{-1}). Both metrics indicate that nutrient diffusion limitations were prevalent in each hydrogel. Average mesh sizes determined by equilibrium swelling theory [25] were measured to be $12 \pm 0.3 \text{ nm}$, $10 \pm 0.3 \text{ nm}$, and $10 \pm 0.8 \text{ nm}$ for PEGDA-PEGTT, PEGVS-PEGTT, and PEGMA-PEGTT, respectively (Fig. S3), which are small enough to cause mass transport limitations during culture [7]. Despite this, cells were able to grow to significant and comparable levels within each hydrogel matrix during the 70-h culture period, showing a 49% to 59% reduction in final carrying capacity compared to bulk culture in equivalent volume and growth media. It was also necessary to verify that hydrogels could provide stable encapsulation of bacteria during culture, as motile bacteria can potentially squeeze through non-uniformities within

hydrogels or degrade liable hydrogel crosslinks for release. OD_{600} readings taken from supernatant culture media (triangles, Fig. 4) were low and did not increase with time, indicating that all hydrogels provided stable cell encapsulation during the growth period. Had cells escaped the hydrogels, OD_{600} readings in the supernatant culture fluid would have increased in a manner comparable to bulk *B. subtilis* cultures (black line, Fig. 4).

Conclusion

These findings advance synthetic hydrogel materials formed with Michael addition click chemistries for integration of viable, functional bacteria into biohybrid systems. The highest levels of uniformity, viability, and single-cell encapsulation found in PEGDA-PEGTT hydrogels make it a strong candidate for use in many applications; however, other considerations may be necessary. For example, acrylate-thiol coupling generates thioester groups at each crosslink that are susceptible to acid or base hydrolysis. If pH stability is desired, PEGVS-PEGTT hydrogels that generate hydrolytically stable thioether sulfone bonds may provide a reasonable alternative. While PEGMA-PEGTT hydrogels in their current form are likely unfeasible for application, recent efforts to slow maleimide-thiol reactions have been reported

Fig. 4 Growth kinetics of *B. subtilis* in bulk culture media (no hydrogel) and *B. subtilis* encapsulated in PEGDA-PEGTT, PEGVS-PEGTT, and PEGMA-PEGTT hydrogels. Triangles represent OD_{600} readings from supernatant culture fluid outside of the hydrogels. Replicate trials were performed at $n \geq 3$



[27], which may improve this crosslinking chemistry for bacteria encapsulation.

Supplementary Information The online version contains supplementary material available at <https://doi.org/10.1557/s43580-024-00940-y>.

Author contributions Moises Gutierrez contributed to Data curation (lead); Formal analysis (lead); Conceptualization (supporting); and Writing—original draft (lead). Jeffrey Reed contributed to Data curation (supporting); Formal analysis (supporting); and Writing—original draft (supporting). Robby McElroy contributed to Data curation (supporting). Ryan Hansen contributed to Conceptualization (lead); Funding acquisition (lead); and Writing—original draft (supporting).

Funding This research was supported by the National Science Foundation (Award 1944791).

Data availability Data will be made available on reasonable request to the corresponding author.

Declarations

Conflict of interest On behalf of all authors, the corresponding author states that there is no conflict of interest.

Open Access This article is licensed under a Creative Commons Attribution 4.0 International License, which permits use, sharing, adaptation, distribution and reproduction in any medium or format, as long as you give appropriate credit to the original author(s) and the source, provide a link to the Creative Commons licence, and indicate if changes were made. The images or other third party material in this article are included in the article's Creative Commons licence, unless indicated otherwise in a credit line to the material. If material is not included in the article's Creative Commons licence and your intended use is not permitted by statutory regulation or exceeds the permitted use, you will need to obtain permission directly from the copyright holder. To view a copy of this licence, visit <http://creativecommons.org/licenses/by/4.0/>.

References

1. M. Afzaal, F. Saeed, A. Ahmed, M. Saeed, H. Ateeq. In Hydrogels as Carrier for the Delivery of Probiotics -Chapter 21 in *Advances in dairy microbial products*, ed. By J. Singh, A. Vyas. (Woodhead Publishing, 2022) 303–315.
2. M. Chaparro-Rodríguez, G. Estrada-Bonilla, J. Rosas-Pérez, M. Gómez-Álvarez, M. Cruz-Barrera, Hydrogel capsules as new approach for increasing drying survival of plant biostimulant gram-negative consortium. *Appl. Microbiol. Biotechnol.* **107**(21), 6671–6682 (2023). <https://doi.org/10.1007/s00253-023-12699-7>
3. C.Y. Tong, C.J.C. Derek, Bio-coatings as immobilized microalgae cultivation enhancement: a review. *Sci. Total. Environ.* **887**, 163857 (2023). <https://doi.org/10.1016/j.scitotenv.2023.163857>
4. A.P. Liu, E.A. Appel, P.D. Ashby, B.M. Baker, E. Franco, L. Gu, K. Haynes, N.S. Joshi, A.M. Kloxin, P.H.J. Kouwer, J. Mittal, L. Morsut, V. Noireaux, S. Parekh, R. Schulman, S.K.Y. Tang, M.T. Valentine, S.L. Vega, W. Weber, N. Stephanopoulos, O. Chaudhuri, The living interface between synthetic biology and biomaterial design. *Nat. Mater.* **21**(4), 390–397 (2022). <https://doi.org/10.1038/s41563-022-01231-3>
5. L.K. Rivera-Tarazona, T. Shukla, K.A. Singh, A.K. Gaharwar, Z.T. Campbell, T.H. Ware, 4D printing of engineered living

6. L.K. Rivera-Tarazona, M. Sivaperuman Kalairaj, T. Corazao, M. Javed, P.E. Zimmern, S. Subashchandrabose, T.H. Ware, Controlling shape morphing and cell release in engineered living materials. *Biomater. Adv.* **143**, 213182 (2022). <https://doi.org/10.1002/adfm.202106843>
7. M.S. Rehmman, K.M. Skeens, P.M. Kharkar, E.M. Ford, E. Maverakis, K.H. Lee, A.M. Kloxin, Tuning and predicting mesh size and protein release from step growth hydrogels. *Biomacromol.* **18**(10), 3131–3142 (2017). <https://doi.org/10.1021/acs.biomac.7b00781>
8. M.W. Tibbitt, A.M. Kloxin, L.A. Sawicki, K.S. Anseth, Mechanical properties and degradation of chain and step-polymerized photodegradable hydrogels. *Macromolecules* **46**(7), 2785–2792 (2013). <https://doi.org/10.1021/ma302522x>
9. N. Fattahi, P.A. Nieves-Otero, M. Masigol, A.J. Van Der Vlies, R.S. Jensen, R.R. Hansen, T.G. Platt, photodegradable hydrogels for rapid screening, isolation, and genetic characterization of bacteria with rare phenotypes. *Biomacromol.* **21**(8), 3140–3151 (2020). <https://doi.org/10.1021/acs.biomac.0c00543>
10. M. Masigol, E.L. Radaha, A.D. Kannan, A.G. Salberg, N. Fattahi, P. Parameswaran, R.R. Hansen, Polymer surface dissection for correlated microscopic and compositional analysis of bacterial aggregates during membrane biofouling. *ACS Appl. Bio Mater.* **5**(1), 134–145 (2022). <https://doi.org/10.1021/acsabm.1c00971>
11. G.M. Gutenberger, O.M. Holgate, W.A. Arnold, J.S. Guest, P.J. Novak, Polyethylene glycol as a robust, biocompatible encapsulant for two-stage treatment of food and beverage wastewater. *Environ. Sci.: Water Res. Technol.* **10**(2), 467–479 (2024). <https://doi.org/10.1039/D3EW00633F>
12. X. Qiao, Z. Liu, Z. Liu, Y. Zeng, Z. Zhang, Optimized immobilization of activated sludge in poly(ethylene glycol) gels by UV technology. *Process Biochem.* **45**(8), 1342–1347 (2010). <https://doi.org/10.1016/j.procbio.2010.05.003>
13. N. Fattahi, J. Reed, E. Heronemus, P. Fernando, R.R. Hansen, P. Parameswaran, Polyethylene glycol hydrogel coatings for protection of electroactive bacteria against chemical shocks. *Bioelectrochemistry* **156**, 108595 (2024). <https://doi.org/10.1016/j.bioelechem.2023.108595>
14. N. Barua, A.M. Herken, K.R. Stern, S. Reese, R.L. Powers, J.L. Morrell-Falvey, T.G. Platt, R.R. Hansen, Simultaneous discovery of positive and negative interactions among rhizosphere bacteria using microwell recovery arrays. *Front. Microbiol.* **11**, 601788 (2021). <https://doi.org/10.3389/fmicb.2020.601788>
15. N. Barua, K.M. Clouse, D.A. Ruiz Diaz, M.R. Wagner, T.G. Platt, R.R. Hansen, Screening the maize rhizobiome for consortia that improve azospirillum brasilense root colonization and plant growth outcomes. *Front. Sustain Food Syst.* **7**, 1106528 (2023). <https://doi.org/10.3389/fsufs.2023.1106528>
16. N. Barua, A.M. Herken, N. Melendez-Velador, T.G. Platt, R.R. Hansen, Photo-addressable microwell devices for rapid functional screening and isolation of pathogen inhibitors from bacterial strain libraries. *Biomechanics* **18**(1), 014107 (2024). <https://doi.org/10.1063/5.0188270>
17. P.M. Kharkar, K.L. Kiick, A.M. Kloxin, Design of thiol- and light-sensitive degradable hydrogels using michael-type addition reactions. *Polym. Chem.* **6**(31), 5565–5574 (2015). <https://doi.org/10.1039/C5PY00750J>
18. K.S. Anseth, H.-A. Klok, Click chemistry in biomaterials, nanomedicine, and drug delivery. *Biomacromol.* **17**(1), 1–3 (2016). <https://doi.org/10.1021/acs.biomac.5b01660>
19. D.P. Nair, M. Podgórski, S. Chatani, T. Gong, W. Xi, C.R. Fenoli, C.N. Bowman, The thiol-michael addition click reaction: a powerful and widely used tool in materials chemistry. *Chem. Mater.* **26**(1), 724–744 (2014). <https://doi.org/10.1021/cm402180t>

20. R. Saberi Riseh, M. HassaniSaadi, M. Vatankhah, F. Soroush, R.S. Varma, Nano/microencapsulation of plant biocontrol agents by chitosan, alginate, and other important biopolymers as a novel strategy for alleviating plant biotic stresses. *Int. J. Biol. Macromol.* **222**, 1589–1604 (2022). <https://doi.org/10.1016/j.ijbio mac.2022.09.278>
21. L. Tu, Y. He, H. Yang, Z. Wu, L. Yi, Preparation and characterization of alginate-gelatin microencapsulated bacillus subtilis SL-13 by emulsification/internal gelation. *J. Biomater. Sci. Polym. Ed.* **26**(12), 735–749 (2015). <https://doi.org/10.1080/09205063.2015.1056075>
22. X. Liu, M.E. Inda, Y. Lai, T.K. Lu, X. Zhao, Engineered living hydrogels. *Adv. Mater.* **34**(26), 2201326 (2022). <https://doi.org/10.1002/adma.202201326>
23. E.R. Morton, C. Fuqua, Laboratory maintenance of agrobacterium. *CP Microbiol.* (2012). <https://doi.org/10.1002/9780471729259.mc03d01s24>
24. N. Fattahi, N. Barua, A.J. Van Der Vlies, R.R. Hansen, Photodegradable hydrogel interfaces for bacteria screening, selection, and isolation. *JoVE* (2021). <https://doi.org/10.3791/63048>
25. T. Canal, N.A. Peppas, Correlation between mesh size and equilibrium degree of swelling of polymeric networks. *J. Biomed. Mater. Res.* **23**(10), 1183–1193 (1989). <https://doi.org/10.1002/jbm.820231007>
26. Thermo-Fisher Scientific. LIVE/DEAD™ BacLight™ Bacterial Viability Kits. Revised 15-July-2004.
27. J. Errington, L.T.V.D. Aart, Microbe profile: bacillus subtilis: model organism for cellular development, and industrial workhorse: this article is part of the microbe profiles collection. *Microbiology* **166**(5), 425–427 (2020). <https://doi.org/10.1099/mic.0.000922>
28. C. Echalié, L. Valot, J. Martinez, A. Mehdi, G. Subra, Chemical crosslinking methods for cell encapsulation in hydrogels. *Mater. Today Commun.* **20**, 100536 (2019). <https://doi.org/10.1016/j.mtcomm.2019.05.012>
29. L.E. Jansen, L.J. Negrón-Piñero, S. Galarza, S.R. Peyton, Control of thiol-maleimide reaction kinetics in peg hydrogel networks. *Acta Biomater.* **70**, 120–128 (2018). <https://doi.org/10.1016/j.actbio.2018.01.043>
30. E.R. Ruskowitz, C.A. DeForest, Photoresponsive biomaterials for targeted drug delivery and 4D cell culture. *Nat. Rev. Mater.* **3**(2), 17087 (2018). <https://doi.org/10.1038/natrevmats.2017.87>

Publisher's Note Springer Nature remains neutral with regard to jurisdictional claims in published maps and institutional affiliations.